Materials Research Bulletin 46 (2011) 190–193

Contents lists available at ScienceDirect

Materials Research Bulletin

journal homepage: www.elsevier.com/locate/matresbu

The crystal and magnetic structure of Ti-substituted $LaCrO_3$

A. Martinelli [a,*], M. Ferretti [a,b], M.R. Cimberle [c], C. Ritter [d]

[a] CNR-SPIN, C.so Perrone 24, 16152 Genova, Italy
[b] Dipartimento di Chimica e Chimica Industriale, Università di Genova, Via Dodecaneso 31, 16146 Genova, Italy
[c] CNR-IMEM, Via Dodecaneso 33, 16146, Genova, Italy
[d] Institute Laue – Langevin, 6 rue Jules Horowitz, 38042 Grenoble Cedex 9, France

ARTICLE INFO

Article history:
Received 10 March 2010
Received in revised form 20 September 2010
Accepted 10 November 2010
Available online 18 November 2010

Keywords:
A. Oxides. A. Magnetic materials
C. Neutron scattering
D. Crystal structure
D. Magnetic properties

ABSTRACT

The crystal and magnetic structures of $LaCrO_3$ and $La(Cr_{0.90}Ti_{0.10})O_3$ have been investigated between 5 and 350 K by means of neutron powder diffraction and DC magnetic measurements. Both compounds are characterized by an antiferromagnetic G_x-type ordering at low temperature. Structural features suggest the occurrence of Ti in the tetra-valent state. Despite the mixed valence induced by Ti-substitution leading to the occurrence of the Jahn–Teller species Cr^{2+}, no evidence for long range ferromagnetism can be detected. On account of a miscibility gap, a higher degree of Ti-substitution at the Cr site cannot be achieved; as a consequence the solid state solubility of Ti in $LaCrO_3$ at 1573 K has been ascertained.
© 2010 Elsevier Ltd. All rights reserved.

1. Introduction

Mixed valence at the Mn-site is at the basis of several interesting properties characterizing the class of compounds referred to as manganites. Depending on the relative amounts of both rare-earth and alkaline earth at the *A* site of the perovskite-type structure $AMnO_3$, different ratios of the Mn^{3+} and Mn^{4+} cationic species can be obtained, resulting in compounds with different structural, magnetic and conductive properties. Mn^{4+} and Mn^{3+} are characterized by a different external electronic configuration, t_{2g}^3 and respectively, this latter inducing a Jahn–Teller distortion due to the degeneracy removal at the e.g. electronic levels. The same electronic configurations could in principle be obtained also in mixed valence chromites hosting Cr^{2+} and Cr^{3+}. For this it is necessary to substitute Cr^{3+} by a tetravalent ion such as Ti^{4+} in rare earth chromites.

Ti-substituted $LaCrO_3$ compounds have been studied in the past, but none of these investigations was supported by an accurate structural characterization of the products and, in addition, the limit solid state solubility of Ti in $LaCrO_3$ has never been defined. Devi and Rao [1] claimed the synthesis at 1123 K of $La(Cr_{1-x}Ti_x)O_3$ compounds with $0 \leq x \leq 0.5$; despite the high level of substitution the samples displayed similar diffraction patterns as well as EPR and IR spectra. Tsukuda et al. [2,3] report the synthesis of compounds with nominal composition up to $x \leq 0.3$, even though notable, but not quantified, amount of secondary $La_2Ti_2O_7$ are observed in the diffraction patterns.

A different kind of mixed valence at the Cr-site could be obtained by creating vacancies at the rare earth site, thus inducing the coexistence of Cr^{3+} with Cr^{4+}; in this context the synthesis of La-deficient $LaCrO_3$ has been claimed by Iliev et al. [4] based on elemental content analysis, resulting in a [La]/[Cr] ratio of 0.95–0.97. Ong et al. [5] report that the green colour of pure $LaCrO_3$ should turn to yellow brownish in case of La or O deficiencies.

With the aim to induce both Cr^{2+}/Cr^{3+} and Cr^{3+}/Cr^{4+} mixed valence in chromites we tried to prepare two samples, the former with Ti-substitution, the latter with La deficiencies.

2. Experimental

Two samples were synthesized by means of a solid state reaction carried out at high temperature in air, heating powder mixtures of high purity binary oxides (La_2O_3 99.99% Alfa Aesar; Cr_2O_3 99.997% Alfa Aesar; TiO_2 99.999% Aldrich). Two thermal treatments at 1573 K for 15 h with intermediate grinding were carried out. The former sample was prepared with an excess of TiO_2 so as to induce mixed valence of the Cr species by alio-valent substitution. After reaction this sample is characterized by a light green colour. The latter sample was prepared using an excess of Cr_2O_3, in order to obtain a compound characterized by vacancies at the La site, similar to those obtained by Iliev et al. [4].

Neutron powder diffraction (NPD) data were collected at the Institute Laue Langevin (Grenoble, France) using the D1A diffractometer ($\lambda = 1.91$ Å); diffraction patterns were collected

* Corresponding author. Tel.: +39 0106598722; fax: +39 0106598732.
E-mail address: amartin@chimica.unige.it (A. Martinelli).

0025-5408/$ – see front matter © 2010 Elsevier Ltd. All rights reserved.
doi:10.1016/j.materresbull.2010.11.016

between 5 and 350 K. Rietveld refinement of NPD data was carried out using the program FULLPROF [6]; by means of a NAC standard an instrumental resolution file was obtained and applied during refinements in order to detect micro-structural contributions to the NPD peak shape. The diffraction lines were modelled by a Thompson-Cox-Hastings pseudo-Voigt peak shape function convoluted with an axial divergence asymmetry function. The background was fitted by a fifth-order polynomial. The following parameters were refined in the last cycle of calculation: the overall scale factor; the background (five parameters of the 5th order polynomial); 2θ–zero; the unit cell parameters; the specimen displacement; the reflection–profile asymmetry; the Wyckoff positions not constrained by symmetry; the isotropic thermal parameters B; the anisotropic strain parameters.

Zero field cooled (ZFC) and field cooled (FC) DC magnetic measurements between 5 and 330 K were carried out using a Quantum Design SQUID magnetometer.

3. Results and discussion

3.1. Ti-substituted sample

After reaction the sample is characterized by a light green colour.

Fig. 1 shows the ZFC–FC curves obtained with an applied field of 5×10^{-2} T; the ZFC curve shows a quite sharp peak at $T_{AFM} \sim 289$ K, signing the occurrence of an antiferromagnetic (AFM) ordering at the Cr site. At the same temperature the FC curve shows a sudden increase, suggesting the onset of a ferromagnetic (FM) signal. Below T_{AFM} the two curves separate and a large hysteresis occurs. Below ~50 K in both ZFC and FC curves the magnetization increases on cooling, suggesting a paramagnetic behaviour, a feature that is not observed in pure $LaCrO_3$ [7].

NPD diffraction reveals that $La(Cr_{1-x}Ti_x)O_3$ crystallizes in the *Pnma* space group at room temperature and no evidence for a structural transition can be detected in the whole inspected temperature range; faint peaks of a secondary phase, identified as $La_2Ti_2O_7$, are also present. Structural data at 5 K and 300 K obtained after Rietveld refinement are reported in Table 1. Fig. 2 shows a Rietveld refinement plot obtained using data collected at 5 K, selected as representative. $La_2Ti_2O_7$ constitutes about 10% of the sample mass. In order to check the effective Ti content in the perovskitic phase, the relative occupancies of both Cr and Ti were refined; in addition the occupancy at the O sites was also checked. No significant variation from the stoichiometric value was detected for oxygen while the cation refinement lead to the effective composition of $La(Cr_{0.90}Ti_{0.10})O_3$. This composition marks the highest degree of Ti-substitution that can be attained at the Cr site in $LaCrO_3$ at the reaction temperature (1573 K). Resulting from the charge compensation the $[Cr^{2+}]/[Cr^{3+}]$ ratio should be equal to ~0.11.

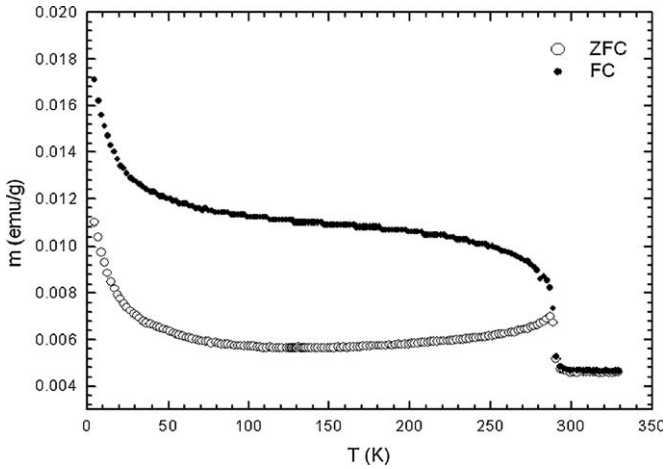

Fig. 1. ZFC–FC curves of La(Cr0.90Ti0.10)O_3.

Table 1
Structural data at 5 K and 300 K obtained from the Rietveld refinement of $LaCrO_3$ and $La(Cr_{0.90}Ti_{0.10})O_3$; both compounds crystallize in the *Pnma* space group: La at 4*c*, Cr and Ti at 4*b*, O(1) at 4*c*, O(2) at 8*d* sites.

		$La(Cr_{0.90}Ti_{0.10})O_3$		$LaCrO_3$	
		5 K	300 K	5 K	300 K
a (Å)		5.4768(1)	5.4872(1)	5.4752(1)	5.4856(1)
b (Å)		7.7539(2)	7.7690(2)	7.7526(1)	7.7677(1)
c (Å)		5.5096(1)	5.5232(1)	5.5088(1)	5.5225(1)
La	x	0.0189(2)	0.0165(5)	0.0212(2)	0.0183(2)
	z	0.9958(3)	0.9972(5)	0.9953(3)	0.9961(2)
O(1)	x	0.4922(4)	0.4931(8)	0.4922(3)	0.4930(5)
	z	0.0636(3)	0.0629(6)	0.0655(3)	0.0650(4)
O(2)	y	0.2259(2)	0.2277(5)	0.2250(2)	0.2260(2)
	z	0.5354(2)	0.5350(3)	0.5355(1)	0.5354(2)
		0.2269(2)	0.2291(4)	0.2253(2)	0.2266(3)
μ_B (Cr)		2.55(2)	/	2.51(2)	/
R_{Bragg} (%)		2.67	4.33	2.10	3.14
R_f (%)		2.13	3.45	1.74	2.66
R_{Magn} (%)		3.72	/	4.97	/

AFM peaks arise between 300 K and 275 K and their intensities progressively increase on cooling. The magnetic propagation vector was determined to be $k = (0,0,0)$. Symmetry analysis was used to determine the possible magnetic ordering at the Cr sublattice, the allowed irreducible representations [8] leading to allowed types of spin ordering were checked with the experimental data. The spins on the Cr-site order in a magnetic structure of the antiferromagnetic G_x-type as displayed in the inset of Fig. 2. As mentioned before, Cr^{2+} and Cr^{3+} are characterized by the same electronic configuration as Mn^{3+} and Mn^{4+}, respectively. According to the semi-covalent model [9] in perovskite-type compounds the magnetic coupling between two Mn^{4+} ions is AFM, whereas that between Mn^{3+} and Mn^{4+} results in FM. In analogy the coupling between Cr^{3+} is AFM, whereas that between Cr^{3+} and Cr^{2+} is FM. Consequently the magnetic coupling at the Cr sub-lattice should be predominantly AFM, since it is mainly constituted of Cr^{3+}. Locally, where coupling between Cr^{3+} and Cr^{2+} takes place, the magnetic

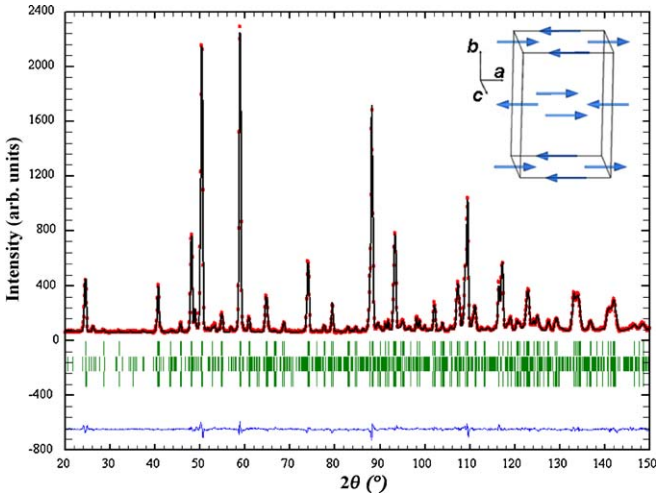

Fig. 2. Rietveld refinement plot of the NPD data collected on Ti-substituted $LaCrO_3$ at 5 K; the inset shows the antiferromagnetic G_x-type structure occurring at the Cr sub-lattice.

moment of Cr^{2+} should be aligned FM with those of the neighbouring Cr^{3+} ions. This scenario explains the simultaneous onset of FM and AFM characters observed in the magnetization curves below T_{AFM}.

3.2. La-deficient sample

The colour of this sample after reaction is deep emerald green, thus different from the yellow brownish expected on the basis of what is reported in Ref. [5]. NPD diffraction reveals the presence of unreacted Cr_2O_3 as a secondary phase; structural data at 5 K and 300 K obtained after Rietveld refinement are reported in Table 1. In order to check for La vacancies leading to a variation of the Cr valence, occupancies at the La and O sites were refined. The refinements reveal that vacancies have neither been obtained at the La site nor at the O sites. Consequently the sample has to be looked upon as being constituted of a mixture of primary $LaCrO_3$ phase and minor amounts of Cr_2O_3 (about 10% mass) that does not affect the quality of the refinement of the primary phase. On the basis of these results the possibility to form vacancies at the rare earth site can be considered debatable. As the sample preparation was carried out under thermodynamic equilibrium conditions, it can be concluded that the possible occurrence of vacancies at La-site occurs under a metastable state. Structural data for $LaCrO_3$ at 5 K and 300 K are reported in Table 1 and are in good agreement with those reported by Khattak and Cox [10]. The phase exhibits the expected behaviour, with magnetic peaks arising between 300 K and 275 K and a progressive increase of their intensities with cooling. The Cr spins order in this compound as well according to an antiferromagnetic G_x-type structure.

Note that the difference among the lattice parameters of our samples at 300 K is larger than that observed by Devi and Rao [1] comparing $La(Cr_{0.95}Ti_{0.05})O_3$ with $La(Cr_{0.60}Ti_{0.40})O_3$, thus questioning the real stoichiometry of the samples analyzed by these authors.

3.3. Discussion

$LaCrO_3$ and $LaTiO_3$ [11] are isostructural, both crystallizing at room temperature in the orthorhombic *Pnma* space group; hence a large solid state solubility between these two end-members could be expected. In this case Ti should retain the tri-valent state when dissolved into $LaCrO_3$ and as a consequence could not induce mixed valence at Cr site. Conversely previous investigations on Ti substitution in $LaCrO_3$ suggest the occurrence of the tetra-valent state for this cationic species. In fact it was argued that the decrease of resistivity taking place by increasing the Ti content in $LaCrO_3$ was originated by the occurrence of Ti^{4+} [1]; also Tsukuda et al. [2] assumed tetra-valent state of Ti in their samples. The limited solid state solubility of Ti in $LaCrO_3$ that we ascertained in our samples is indicative of the fact that this cationic species is effectively in the tetra-valent state. In fact Ti^{4+} (ionic radius: IR = 0.605 Å) induces a mixed valence state of Cr by the formation of Cr^{2+} (IR = 0.8 Å), thus reducing the thermodynamic stability of the phase; as the amount of Cr^{2+} increases lattice strains are enhanced, also on account of the Jahn–Teller character of this cationic species. Conversely if Ti^{3+} should occur the instability of the solid solution could not be ascribed to a steric reason, since Ti^{3+} and Cr^{3+} are characterized by quite similar values of IR (0.67 Å and 0.615 Å, respectively; IR values are reported in Ref. [12]). This is also confirmed by the fact that the Goldschmidt's tolerance factor is about the same when calculated assuming Ti in the tri- or tetra-valent state.

The results of the bond valence sum (BVS) calculations [13] carried out using the refined cell data are reported in Table 2. An excellent agreement between the nominal and the calculated values is obtained for both samples at La, O(1) and O(2) sites, whereas the value at the transition metal site exceeds the expected value. The difference between the BVS and the nominal valence (discrepancy) is generally $\leq$0.1 vu (vu: valence unit), unless the occurrence of lattice strains determines the stretching or compression of the bonds; larger values of the discrepancy are thus indicative of strained bonds [13]. The occurrence of Ti^{4+} can be ascribed to the fact that the *B*-O bond lengths are almost the same in $La(Cr_{0.90}Ti_{0.10})O_3$ and $LaCrO_3$ ($\sim$1.97 Å; Table 3), whereas in pure $LaTiO_3$ they range around 2.03 Å [11]. As a consequence Ti can accommodate the large negative charge of the neighbouring O atoms only by oxidizing to the tetra-valent state when dissolved into $LaCrO_3$ (in this way the IR of Ti reduces as well). In fact using the experimental bond lengths and the BV parameters of Ti^{3+} and Ti^{4+} the BVS result 3.6 vu and 3.9 vu, respectively.

Table 2
BVS values at the different atomic sites.

	BVS (vu)	
	$La(Cr_{0.90}Ti_{0.10})O_3$	$LaCrO_3$
La	2.95	2.99
B	3.14	3.13
O(1)	2.04	2.02
O(2)	2.05	2.04

Table 3
B-O bond lengths in $LaCrO_3$ and $La(Cr_{0.90}Ti_{0.10})O_3$.

	$La(Cr_{0.90}Ti_{0.10})O_3$		$LaCrO_3$	
	5 K	300 K	5 K	300 K
B-O(1) [Å] × 2	1.970(1)	1.9734(6)	1.972(1)	1.9752(4)
B-O(2) [Å] × 2	1.973(1)	1.977(3)	1.970(1)	1.975(2)
B-O(2) [Å] × 2	1.967(1)	1.968(2)	1.970(1)	1.973(2)

The different lattice effects induced by the different valence state of Ti can be quantified by the variance σ^2 of the transition metal site [14]; as a result σ^2 results six times larger when the occurrence of Ti^{4+} is assumed, possibly implying the arising of lattice strains.

Two main results are obtained by this kind of analysis: (1) the BVS at La and O sites confirms that the amount of vacancies is negligible; (2) the transition metal site undergoes lattice strains that slightly increase by Ti substitution on account of the increased σ^2. Note that the both σ^2 and BVS parameter for the *B* site of $La(Cr_{0.90}Ti_{0.10})O_3$ has been calculated by weighting the parameters of the coexisting Cr^{3+}, Cr^{2+} and Ti^{4+} ions.

In this context information on the effect of the Ti-substitution on the micro-structure of the samples was obtained analyzing the broadening of NPD lines (high resolution – D1A data) by means of the Williamson–Hall plot method [15]. Generally, in the case where size effects are negligible and the strain is isotropic, a straight line passing through all the points and through the origin has to be observed, where the slope provides the lattice strain: the higher the slope the higher the strain. If the broadening is not isotropic, size and strain effects along some crystallographic directions can be obtained by considering different orders of the same reflection. In our case, for each sample, the size contribution is negligible, since a straight line passing through the origin can be traced. Fig. 3 shows the superposition of the Williamson–Hall plots obtained by the micro-structural analysis of the data collected at 300 K on D1A; for clarity only selected diffraction peaks are reported and indexed. This plot clearly indicates that lattice strains are quite anisotropic, mainly oriented along the [0 1 0] and confirms that Ti substitution determines their slight increase, as expected in the case of its occurrence in the tetra-valent state.

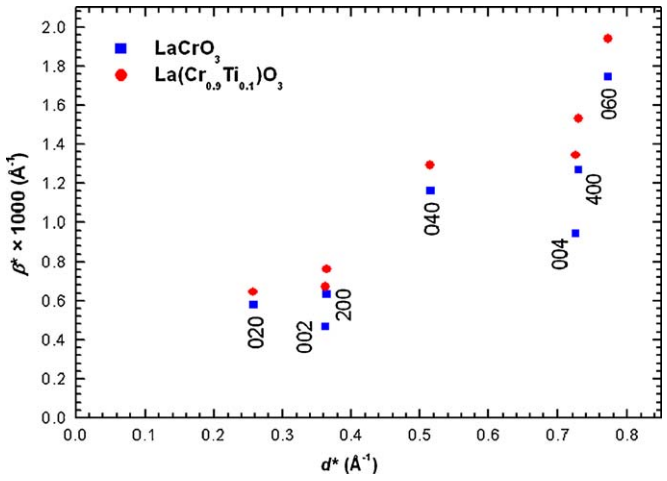

Fig. 3. Superposition of the Williamson–Hall plots obtained by the micro-structural analysis of the data collected at 300 K on D1A; only selected diffraction peaks are reported and indexed.

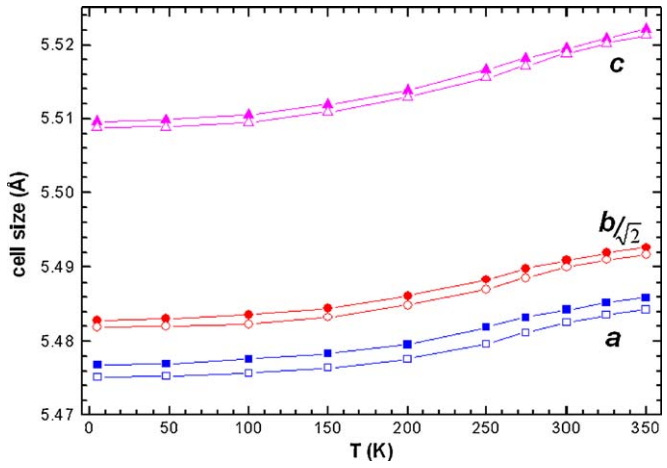

Fig. 4. Evolution of the cell edges between 5 and 300 K; empty and full symbols are for $LaCrO_3$ and $La(Cr0.90Ti0.10)O_3$, respectively. Error bars are smaller than the symbols.

Ti-substitution in $LaCrO_3$ leads to an isotropic increase of the unit cell parameters, as evidenced by the data reported in Table 1 and by their evolution with temperature is reported in Fig. 4. This is consistent with Ti substitution, whatever its oxidation state, that determines a similar as well as slight increase of the average IR at the transition metal site (IR ~0.63 to 0.62 Å). A strong negative deviation from the Vegard's law is observed by plotting the cell parameters of $La(Cr_{0.90}Ti_{0.10})O_3$ and those of the end members.

Fig. 5 shows the evolution of the magnetic moment at the Cr site with temperature: between room temperature and 150 K a more rapid increase is observed in $LaCrO_3$, probably on account of the

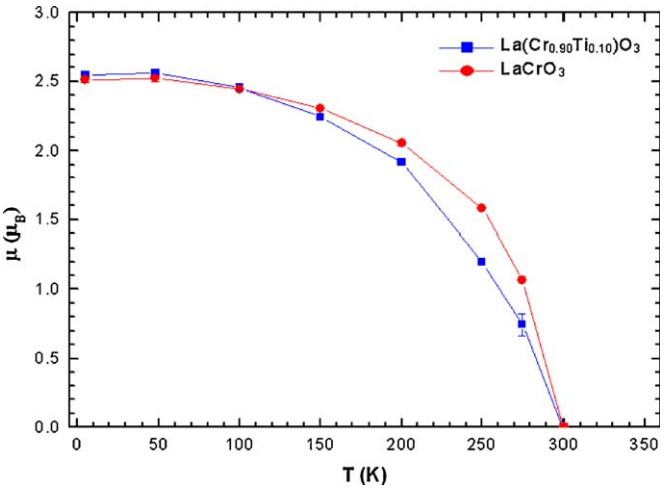

Fig. 5. Dependence of the magnetic moment at the Cr site on temperature.

fact that the presence of Ti^{4+} in the magnetic sub-lattice of $La(Cr_{0.90}Ti_{0.10})O_3$ prevents exchange interactions among neighbouring Cr ions.

4. Conclusions

Attempts to induce mixed valence at the *B* site in $LaCrO_3$ have been carried using two different approaches. Substituting Cr by Ti leads to the formation of $La(Cr_{0.90}Ti_{0.10})O_3$ where structural features determined by neutron diffraction suggest the occurrence of both Cr^{2+} and Cr^{3+}. The attempt to induce La-vacancies at the *A* site and thereby the formation of a Cr^{3+}/Cr^{4+} mixture was not successful. The maximum solid state solubility of Ti in $LaCrO_3$ has been ascertained. The magnetic structure adopted in the Ti-substituted compound in zero magnetic field is not affected by the mixed valence and an antiferromagnetic G_x-type structure is found below 290 K, similar to that detected in the parent compound $LaCrO_3$. Ferromagnetic interactions are, however, mirrored in the field cooled magnetization curves of the Ti-substituted compound.

References

[1] P.S. Devi, M.S. Rao, J. Mater. Sci. Lett. 11 (1992) 226.
[2] H. Tsukuda, Y. Inoue, Y. Uchiyama, J. Ceram. Soc. Jpn. 112 (2004) 167.
[3] H. Tsukuda, Y. Inoue, Y. Uchiyama, J. Ceram. Soc. Jpn. 113 (2005) 353.
[4] M.N. Iliev, A.P. Litvinchuk, V.G. Hadjiev, Y.-Q. Wang, J. Cmaidalka, R.-L. Meng, Y.-Y. Sun, N. Kolev, M.V. Abrashev, Phys. Rev. B 74 (2008) 214301.
[5] K.P. Ong, P. Blaha, P. Wu, Phys. Rev. B 77 (2008) 073102.
[6] J. Rodríguez–Carvajal, Physica B 192 (1993) 55.
[7] N. Sakai, H. Fjellvâg, B.C. Hauback, J. Solid State Chem. 121 (1996) 202.
[8] E.F. Bertaut, Acta Cryst. A24 (1968) 217.
[9] J.B. Goodenough, Phys. Rev. 100 (1955) 564.
[10] C.P. Khattak, D.E. Cox, Mater. Res. Bull. 12 (1977) 463.
[11] M. Eitel, J.E. Greedan, J. Less-Common Met. 116 (1986) 95.
[12] R.D. Shannon, Acta Cryst. A32 (1976) 751.
[13] G.H. Rao, K. Bärner, I.D. Brown, J. Phys: Condens. Matter. 10 (1998) L757–L763.
[14] J.P. Attfield, Chem. Mater. 10 (1998) 3239.
[15] J.I. Langford, D. Louër, E.J. Sonneveld, J.W. Visser, Powder Diffr. 1 (1986) 211.